Electronic Supplementary Material (ESI) for Physical Chemistry Chemical Physics.
This journal is © the Owner Societies 2023

Supplementary Information

Polarization dependent second harmonic generation in peptide crystals: effects of molecular packing†

Sujay Kumar Nandi,[a]‡ *Samrat Ray,*[b]‡ *Bipul Pal,**[b] *and Debasish Haldar**[a]

[a]Department of Chemical Sciences, Indian Institute of Science Education and Research, Kolkata, Mohanpur-741246, West Bengal, India. E-mail: deba_h76@iiserkol.ac.in

[b]Department of Physical Sciences, Indian Institute of Science Education and Research Kolkata, Mohanpur-741246, West Bengal, India. E-mail: bipul@iiserkol.ac.in

Table of contents

Contents	Page No.
1. FT-IR spectra of the peptides. Fig. S1:	S4
2. ORTEP diagram of the Peptide **1** Fig. S2:	S4
3. ORTEP diagram of the Peptide **2** Fig. S3:	S5
4. ORTEP diagram of the Peptide **3** Fig. S4:	S6
5. Hirshfeld surface maps of the Peptide **1** Fig. S5	S7
6. Hirshfeld surface maps of the Peptide **2** Fig. S6	S8
7. Hirshfeld surface maps of the Peptide **3** Fig. S7	S9
8. Square-law dependence of SHG signal Fig. S8	S10
9. Second Harmonic Generation Calculations	S11-S13
10. Synthesis of different peptides. Fig. S9-S32	S14-S29
11. References	S30

Experimental

General: The amino acids were procured from Sigma Chemicals. N,N'-dicyclohexylcarbodiimide and N-hydroxybenzotriazole were purchased from SRL.

Peptide Synthesis: Describe below.

NMR Experiments: All NMR studies were performed on Jeol 400 MHz and Bruker 500 MHz spectrometers at 298 K. Compound concentrations were in the range of 1–10 mM in $CDCl_3$ and DMSO-d_6.

FT-IR Spectroscopy: KBr disk technique solid state FT-IR spectra were obtained with a Perkin Elmer Spectrum RX1 spectrophotometer.

Mass spectrometry: Electrospray ionization (positive-mode) mass spectra of the compounds were recorded on a Q-Tof Micro YA263 high-resolution (Waters Corporation) mass spectrometer.

Absorption Spectroscopy: All absorption spectra were recorded on a Perkin Elmer UV/Vis spectrometer (LAMBDA 35) using a 1 cm path length quartz cell.

Fluorescence Spectroscopy: All fluorescence spectra were recorded on a Perkin Elmer fluorescent spectrometer (LS 55) using a 1 cm path length quartz cell. Slit widths 2.5/2.5 were used.

Single crystal X-ray diffraction study: Intensity data of the reported peptides **p1**, **p2**, and **p3** were collected with molybdenum Kα radiation using Bruker APEX-2 CCD diffractometer. Data were processed using the Bruker SAINT package and the structure solution and refinement procedures were performed using SHELX97. CCDC: 2175161, 2175162 and 2175164 contain the supplementary crystallographic data for peptides **p1**, **p2**, and **p3**, respectively .

Field Emission Scanning Electron Microscopy: FE-SEM has been used to study the morphologies of the three peptides. A drop of sample solution was placed on a clean microscopic glass slide and dried by slow evaporation. The materials were gold-coated, and the micrographs were taken in an FE-SEM apparatus (ZEISS DSM 950 scanning electron microscope).

FT-IR spectra:

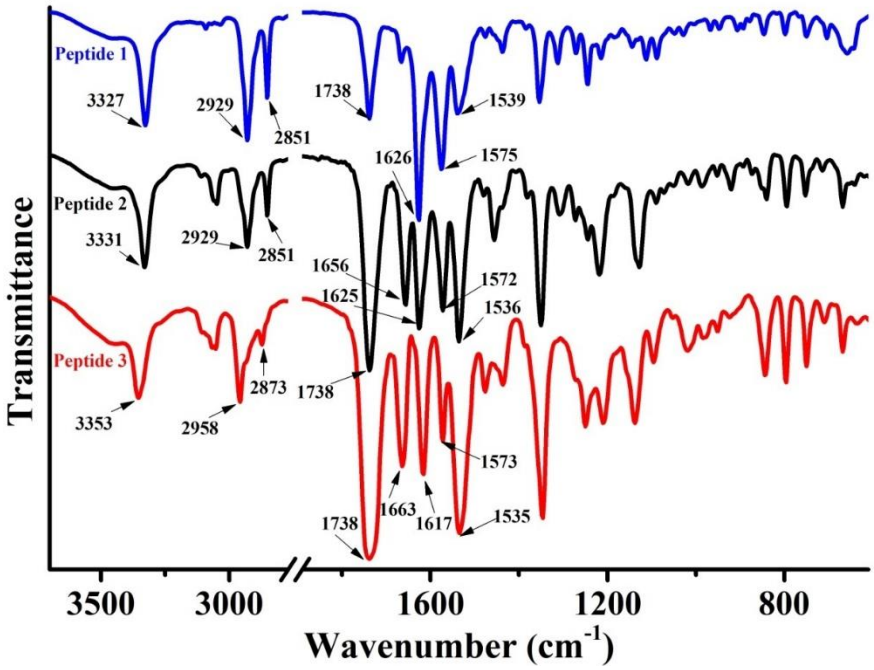

Fig. S1: FT-IR spectrum of the peptides **p1**-**p3**.

Oak Ridge Thermal Ellipsoid Plot (ORTEP) diagram:

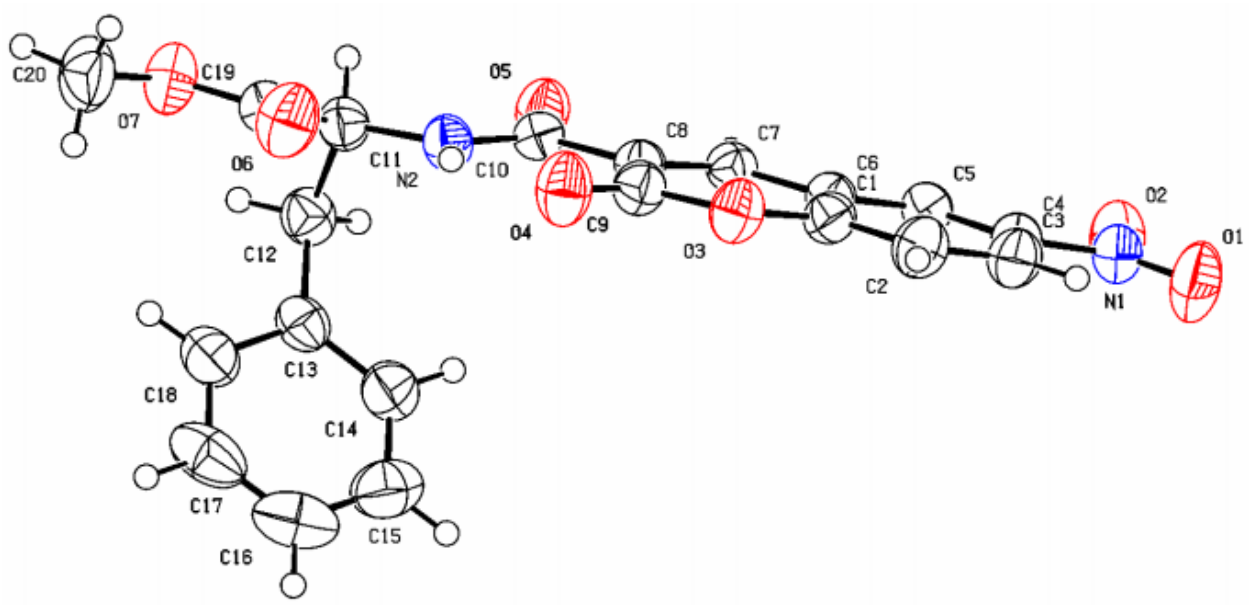

Fig. S2: ORTEP diagram of the Peptide **p1**

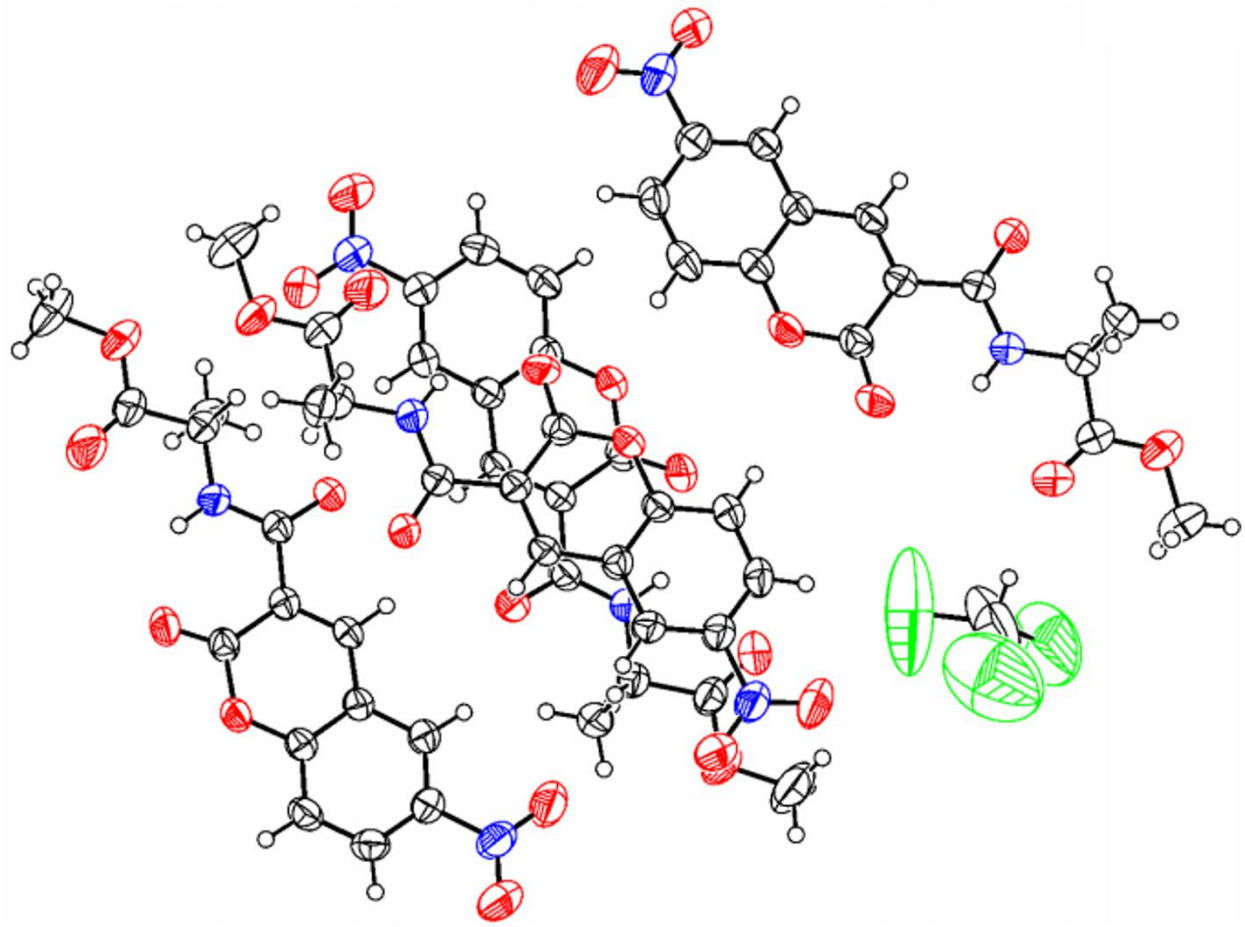

Fig. S3: ORTEP diagram of the Peptide **p2**

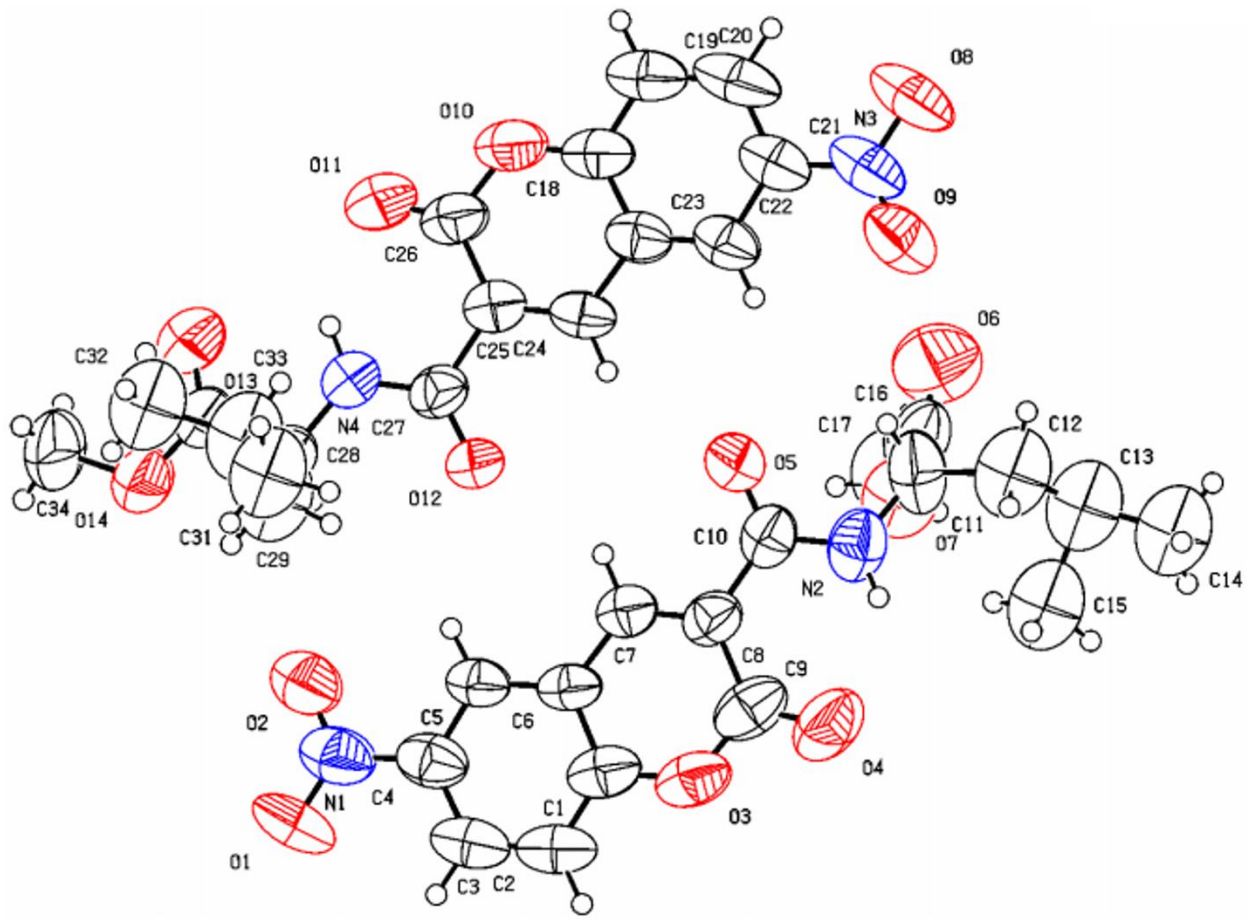

Fig. S4: ORTEP diagram of the Peptide **p3**

Hirshfeld surface maps:

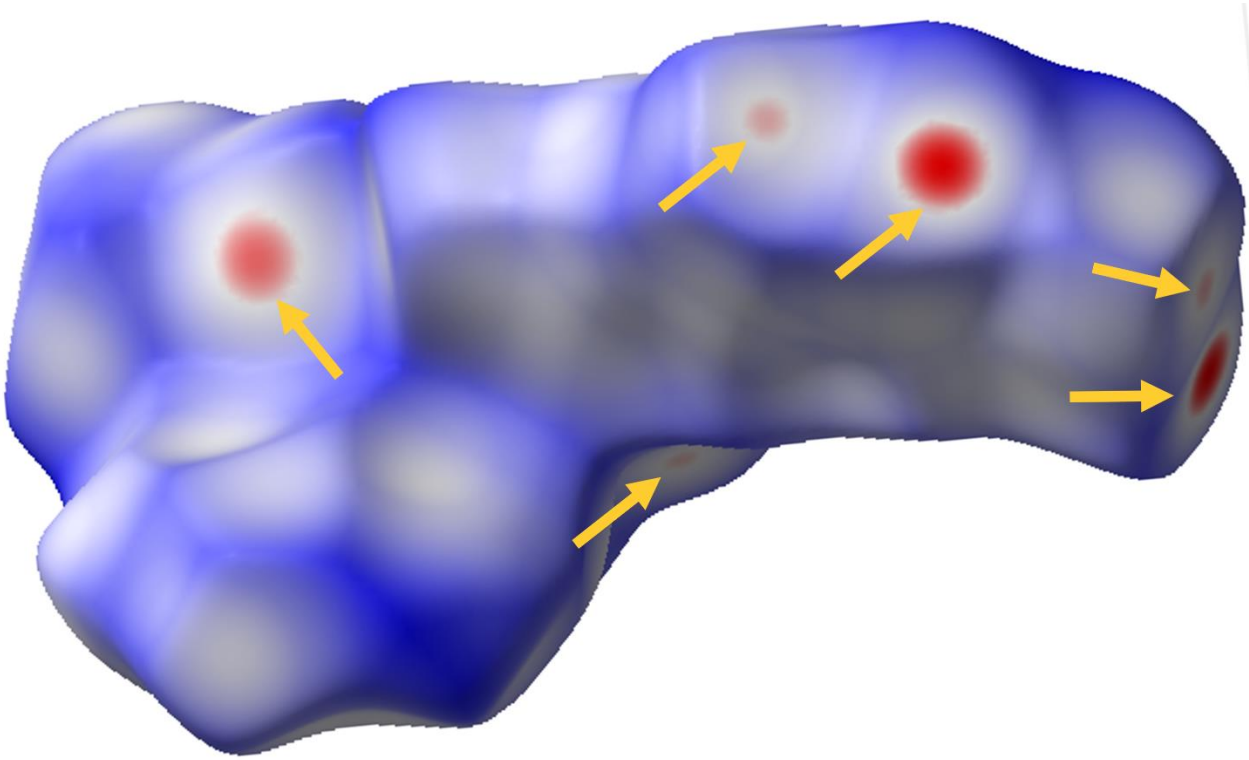

Fig. S5: Hirshfeld surface maps of the Peptide **p1**.

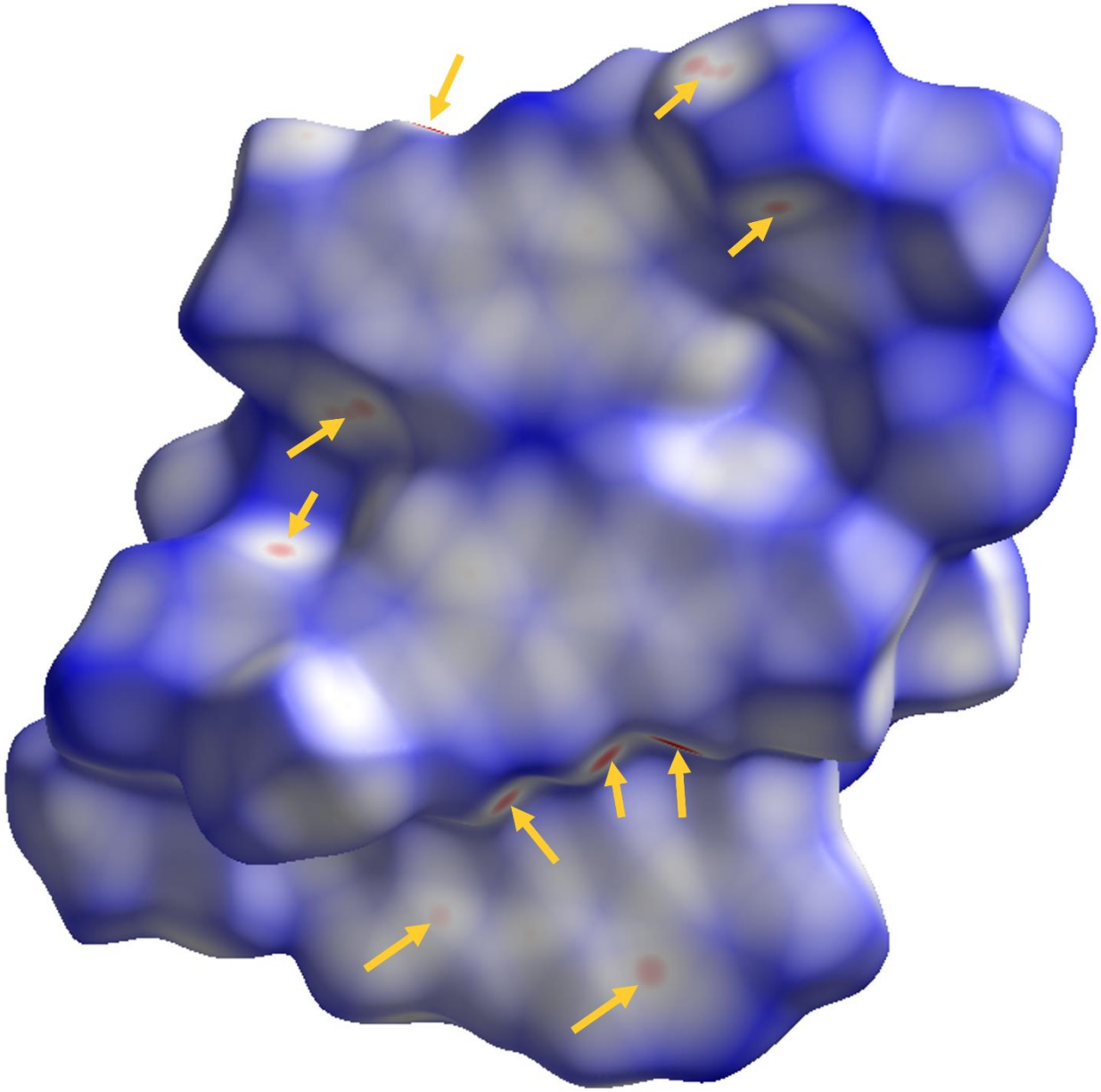

Fig. S6: Hirshfeld surface maps of the Peptide **p2**

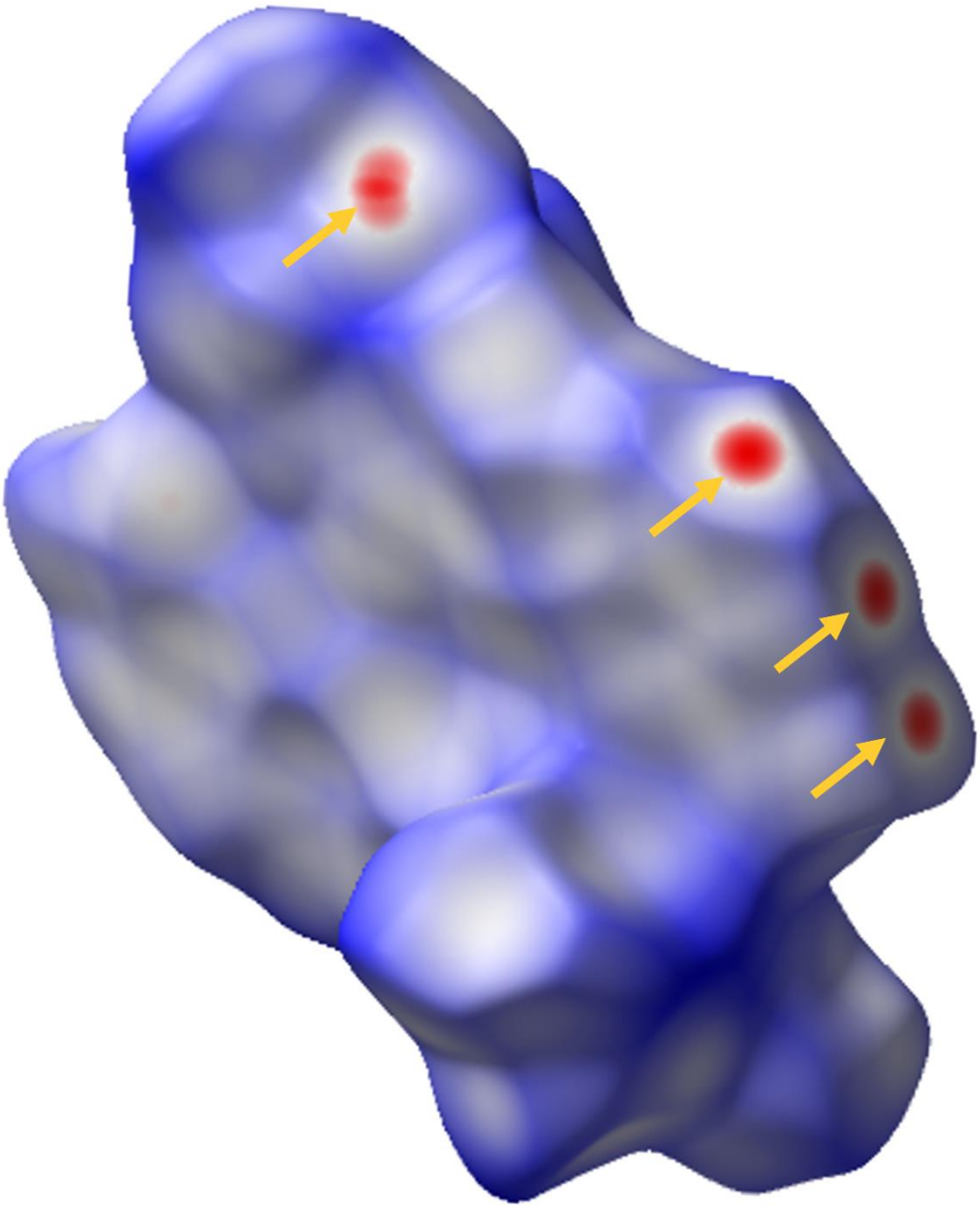

Fig. S7: Hirshfeld surface maps of the Peptide **p3**

Square-law dependence of SHG signal on the input laser intensity:

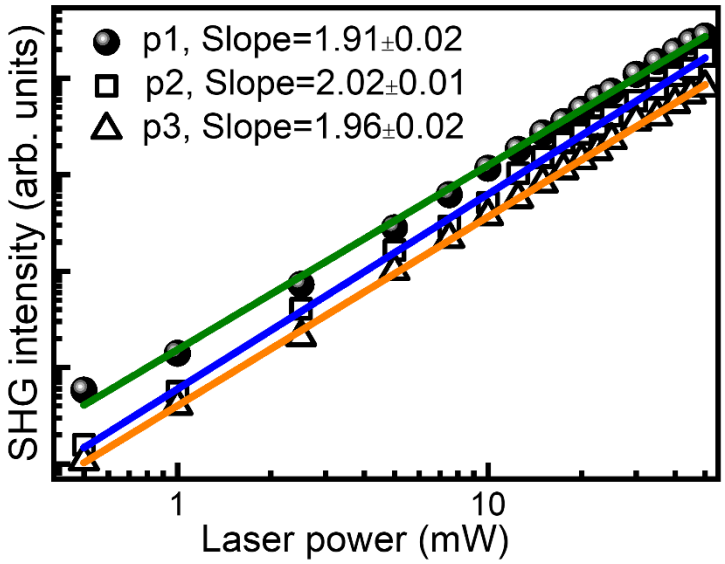

Fig. S8: SHG signal intensity plotted as a function of the input laser power in log-log scale show linear behaviour with slope very close to 2.

Second Harmonic Generation Calculations

The polarization equation considering the second-order susceptibility can be written as,

$$P_i(2\omega = \omega + \omega) = \sum_{j,\,k} \chi_{ijk}^{(2)}(2\omega; \omega, \omega) E_j(\omega) E_k(\omega) \ldots\ldots\ldots (S1)$$

where $\chi_{ijk}^{(2)}$ is the second-order nonlinear susceptibility and is a third-rank tensor composed of 27 components. $\chi_{ijk}^{(2)}$ can be expressed as,

$$\chi_{ijk}^{(2)} = \begin{bmatrix} \chi_{xxx}^{(2)} & \chi_{xxy}^{(2)} & \chi_{xxz}^{(2)} \\ \chi_{xyx}^{(2)} & \chi_{xyy}^{(2)} & \chi_{xyz}^{(2)} \\ \chi_{xzx}^{(2)} & \chi_{xzy}^{(2)} & \chi_{xzz}^{(2)} \end{bmatrix} \begin{bmatrix} \chi_{yxx}^{(2)} & \chi_{yxy}^{(2)} & \chi_{yxz}^{(2)} \\ \chi_{yyx}^{(2)} & \chi_{yyy}^{(2)} & \chi_{yyz}^{(2)} \\ \chi_{yzx}^{(2)} & \chi_{yzy}^{(2)} & \chi_{yzz}^{(2)} \end{bmatrix} \begin{bmatrix} \chi_{zxx}^{(2)} & \chi_{zxy}^{(2)} & \chi_{zxz}^{(2)} \\ \chi_{zyx}^{(2)} & \chi_{zyy}^{(2)} & \chi_{zyz}^{(2)} \\ \chi_{zzx}^{(2)} & \chi_{zzy}^{(2)} & \chi_{zzz}^{(2)} \end{bmatrix}$$

Most commonly in second-order nonlinear optics, the susceptibility $\chi_{ijk}^{(2)}$ is replaced by the so-called d-coefficient, where d can be written as,

$$d_{ijk} = \frac{1}{2}\chi_{ijk}^{(2)} \ldots\ldots (S2)$$

Under symmetry operations allowed for the medium, the d-coefficient must remain unchanged. This reduces the number of independent and nonzero elements as shown in the following.

Intrinsic permutation symmetry: Intrinsic permutation symmetry is a fundamental property of nonlinear susceptibility. Considering principles of time invariance and causality, this symmetry operates universally. This symmetry makes nonlinear optical vector multiplications different from usual vector multiplication - the order of multiplied fields can be altered without affecting the property.

Using this property Eq. S1 can be written as

$$P_i(2\omega = \omega + \omega) = \sum_{j,\,k} \chi_{ikj}^{(2)}(2\omega; \omega, \omega) E_k(\omega) E_j(\omega) \ldots\ldots\ldots (S3)$$

As the $P_i(2\omega = \omega + \omega)$ remains unchanged for both the Eq. S1 and S3, from Eq. S2 we can write,

$$d_{ijk} = d_{ikj} \ldots\ldots\ldots (S4)$$

This property, known as the intrinsic permutation symmetry, serves to contract the last two subscripts of the d tensor and d_{ijk} can be written as d_{il}. The 27 independent components reduce to 18 due to the contraction of the last two subscripts of d-coefficient.

After applying this symmetry operation and designating them numerically we expressed the d-coefficient in Table S1 as follows.

Table S1: Designation of different components of d–coefficient.

$\boldsymbol{i}$		$\boldsymbol{l}$	
Coordinate	Designated by	Coordinate	Designated by
x	1	$j \quad k$	
y	2	$x \quad x$	1
z	3	y $\quad y$	2
		$z \quad z$	3
		$y \quad z = z \quad y$	4
		$z \quad x = x \quad z$	5
		$x \quad y = y \quad x$	6

Thus the d-coefficient can be written as,

$$d_{il} = \begin{bmatrix} d_{11} & d_{12} & d_{13} & d_{14} & d_{15} & d_{16} \\ d_{21} & d_{22} & d_{23} & d_{24} & d_{25} & d_{26} \\ d_{31} & d_{32} & d_{33} & d_{34} & d_{35} & d_{36} \end{bmatrix} \ldots\ldots\ldots (\mathrm{S5})$$

Kleinman symmetry: Kleinman symmetry property can be used when there is no absorption or dispersion at any of the frequencies (ω and 2ω). Then the frequencies can be freely permuted without permuting the corresponding subscripts, and vice versa and the susceptibility remains unchanged. This symmetry operation further reduces the number of independent components of d-coefficient as a few of them become equal to each other. Following this symmetry operation, the equal terms of the d-coefficient have been written in Table 2 as follows.

Table S2: Different components of d–coefficient under Kleinman Symmetry.

Kleinman Symmetry			
d_{21}	d_{211}	d_{121}	d_{16}
d_{25}	d_{231}	d_{123}	d_{14}
d_{26}	d_{212}	d_{122}	d_{12}
d_{31}	d_{311}	d_{131}	d_{15}
d_{32}	d_{322}	d_{232}	d_{24}
d_{34}	d_{323}	d_{233}	d_{23}
d_{35}	d_{331}	d_{133}	d_{13}
d_{36}	d_{312}	d_{123}	d_{14}

Thus after intrinsic permutation symmetry and Kleinman's Symmetry the net polarization equation can be written in matrix form as,[1-3]

$$\begin{bmatrix} P_x(2\omega) \\ P_y(2\omega) \\ P_z(2\omega) \end{bmatrix} = 2\epsilon_0 \begin{bmatrix} d_{11} & d_{12} & d_{13} & d_{14} & d_{15} & d_{16} \\ d_{16} & d_{22} & d_{23} & d_{24} & d_{14} & d_{12} \\ d_{15} & d_{24} & d_{33} & d_{23} & d_{13} & d_{14} \end{bmatrix} \begin{bmatrix} E_x^2(\omega) \\ E_y^2(\omega) \\ E_z^2(\omega) \\ 2E_y(\omega)E_z(\omega) \\ 2E_x(\omega)E_z(\omega) \\ 2E_x(\omega)E_y(\omega) \end{bmatrix} \quad \dots\dots\dots (S6)$$

Additional spatial symmetry properties such as rotation axis and mirror plane symmetries of a nonlinear optical medium can impose additional restrictions on the form of the nonlinear susceptibility tensor. Considering these the d-coefficient for the space group $P_{21\,21\,21}$ can be written as[1–3]

$$d_{il} = \begin{bmatrix} 0 & 0 & 0 & d_{14} & 0 & 0 \\ 0 & 0 & 0 & 0 & d_{14} & 0 \\ 0 & 0 & 0 & 0 & 0 & d_{14} \end{bmatrix} \dots\dots\dots (S7)$$

Similarly for P_{21} and C_2 space group the d-coefficient matrices have the same form and that can be written as[1–3]

$$d_{il} = \begin{bmatrix} 0 & 0 & 0 & d_{14} & 0 & d_{16} \\ d_{16} & d_{22} & d_{23} & 0 & d_{14} & 0 \\ 0 & 0 & 0 & d_{23} & 0 & d_{14} \end{bmatrix} \dots\dots\dots (S8)$$

Peptide Synthesis:

The reported peptides were synthesized by conventional solution-phase methodology using a racemization-free fragment condensation strategy (Scheme 1). For N-terminal protection, nitrocoumarin was used and the C- terminal was protected as a methyl ester. Couplings were mediated by dicyclohexylcarbodiimide/1-hydroxybenzotriazole (DCC/ HOBt). The product was purified by column chromatography using the silica (100-200-mesh size) gel as a stationary phase and n-hexane-ethyl acetate mixture as eluent. The final compounds were fully characterized by 400 MHz & 500 MHz ^{1}H NMR spectroscopy, ^{13}C NMR spectroscopy, mass spectrometry and IR spectroscopy.

Synthetic Scheme:

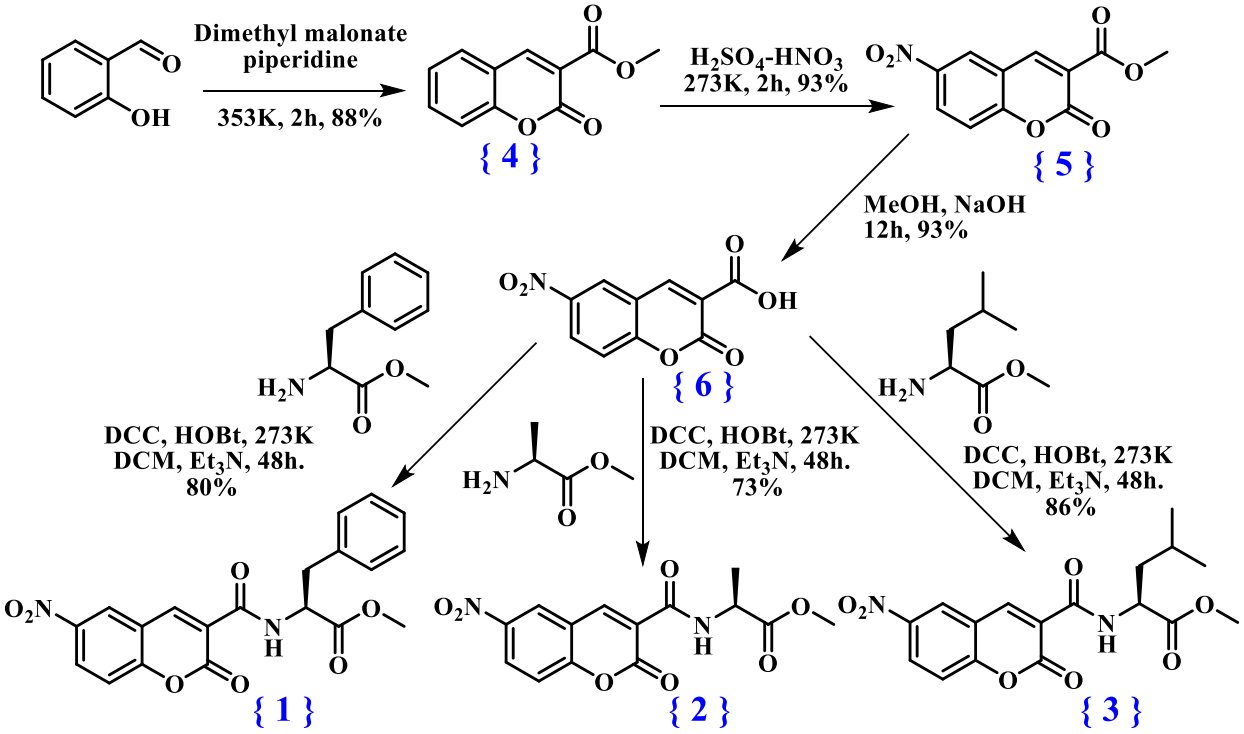

Scheme 1: Synthetic route of the peptide **1**, **2** & **3**.

Synthetic Procedure:

(a). Synthesis of coumarin-3-carboxylic acid methyl ester (4):

2 mL (18.6 mmol) of salicylaldehyde, 2.18 mL (19 mmol) of dimethyl malonate and 200 µL of piperidine were taken in a 50 mL round bottom flux and refluxed at 80 ºC for 2 h with continuous stirring. The reaction mixture was cooled to room temperature. After that ethyl acetate and water

were added and shaken vigorously. The Ethyl acetate layer was collected and dried over anhydrous Na_2SO_4. The products were purified by column chromatography using silica (100-200 mesh size) gel as a stationary phase and an ethyl acetate: n-hexane (1:3) as an eluent.

Yield: 3.12 g (15.20 mmol, 88.25%).

^{1}H NMR (400 MHz, $CDCl_3$, δ in ppm, 298K): 8.47-8.44 (s, 1H, Ar-H), 7.53-7.50 (m, 2H, Ar-H), 7.20-7.24 (m, 2H, Ar-H), 3.81 (s, 3H, -OCH_3). ^{13}C NMR (100 MHz, $CDCl_3$, δ in ppm, 298K): 162.66, 158.13, 155.08, 147.99, 143.59, 128.67, 126.13, 119.23, 118.12, 117.78, 52.73. HR-ESI-MS (m/z): $[M+H]^+$ calculated for $C_{11}H_9O_4$ = 205.0423, found 205.1759.

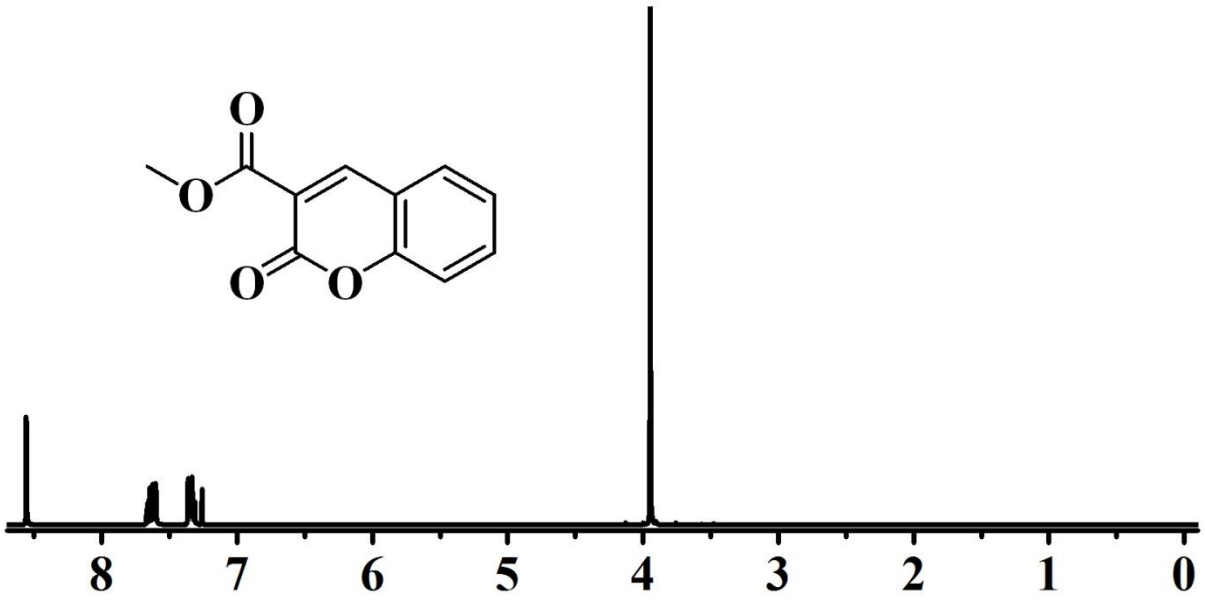

Fig. S9: ^{1}H NMR (400 MHz, $CDCl_3$, δ in ppm, 298K) spectra of Compound **4**.

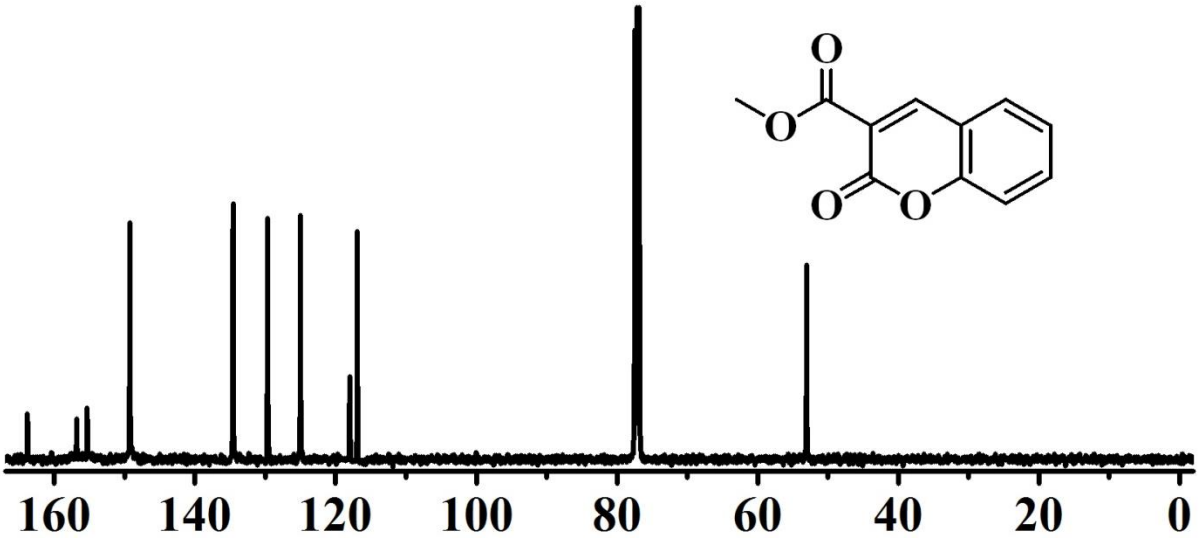

Fig. S10: ^{13}C NMR (100 MHz, $CDCl_3$, δ in ppm, 298K) spectra of Compound **4**.

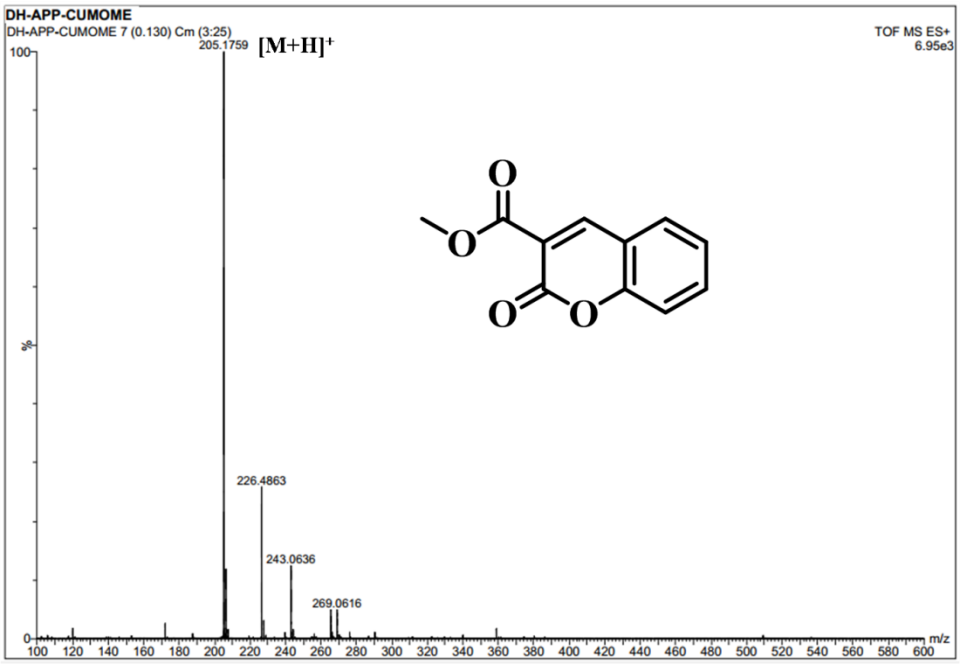

Fig. S11: Mass spectrum of Compound **4**.

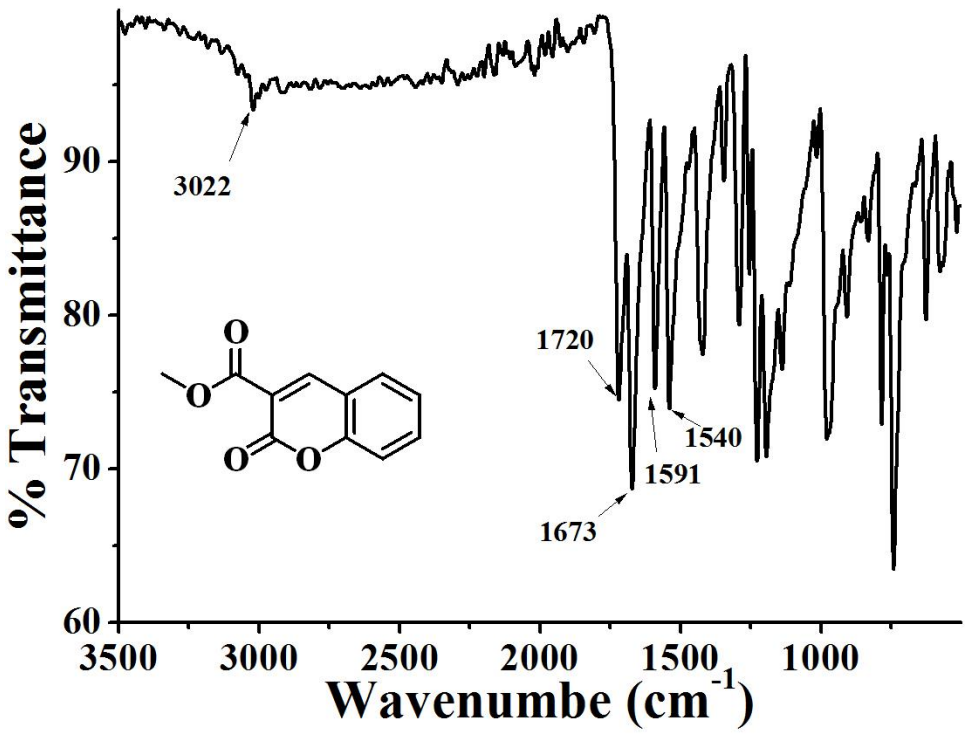

Fig. S12: FT-IR spectrum of Compound **4**.

(b). Synthesis of 6-nitro coumarin-3-carboxylic acid methyl ester (5):

3.00 g (15.78 mmol) of compound **4** was dissolved in 7.90 mL of conc. H_2SO_4 and stirred at 0 ^oC for 15 min. Then a mixture of 3.00 mL (55.46 mmol) nitric acid and 3.65 mL (58.65 mmol) H_2SO_4 was added dropwise and stirred for 1 h at the temperature range 0-5 ^oC. Then the reaction mixture was poured into ice-water and filtered. The residue was washed with fresh water repetitively and dried. The product was purified by column chromatography using silica (100-200 mesh) gel and ethyl acetate:n-hexane (1:2) as an eluent.

Yield: 3.65 g (14.58 mmol, 92.82%).

^{1}H NMR (400 MHz, DMSO-d_6, δ in ppm, 298K): 8.94-8.91 (s, 2H, Ar-H), 8.54-8.53 (m, 1H, Ar-H), 7.66-7.64 (m, 1H, Ar-H), 3.86-3.83 (s, 3H, -OCH_3). ^{13}C NMR (100 MHz, DMSO-d_6, δ in ppm, 298K): 162.83, 158.10, 148.95, 145.94, 128.62, 126.09, 121.65, 118.19, 117.64, 111.03, 52.31. HR-ESI-MS (m/z): $[M+H]^+$ calculated for $C_{11}H_8NO_6$ = 250.0273, found 250.0944.

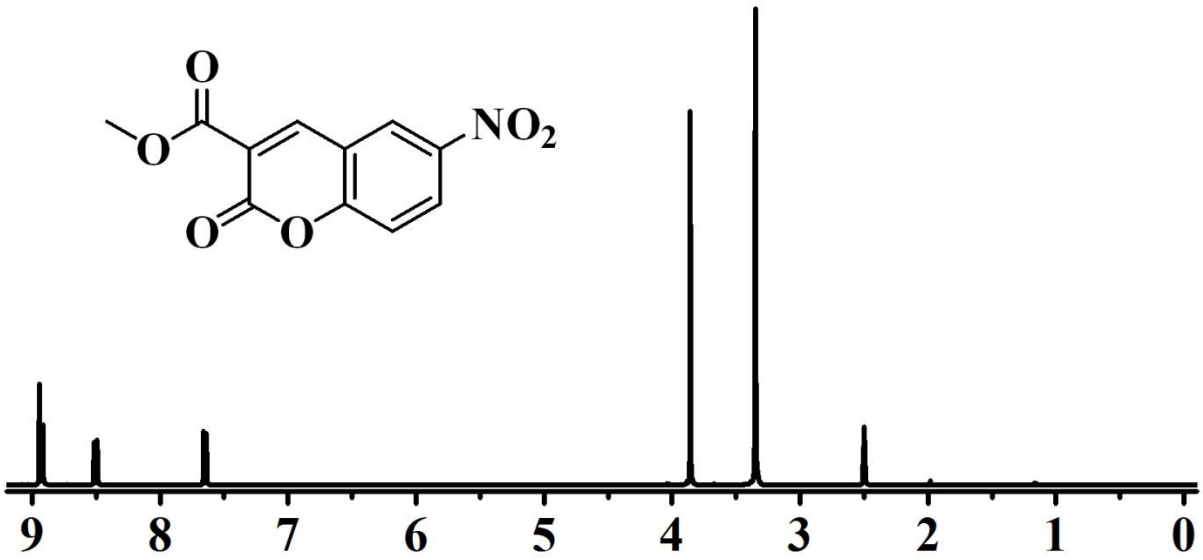

Fig. S13: ^{1}H NMR (400 MHz, DMSO-d_6, δ in ppm, 298K) spectra of Compound **5**.

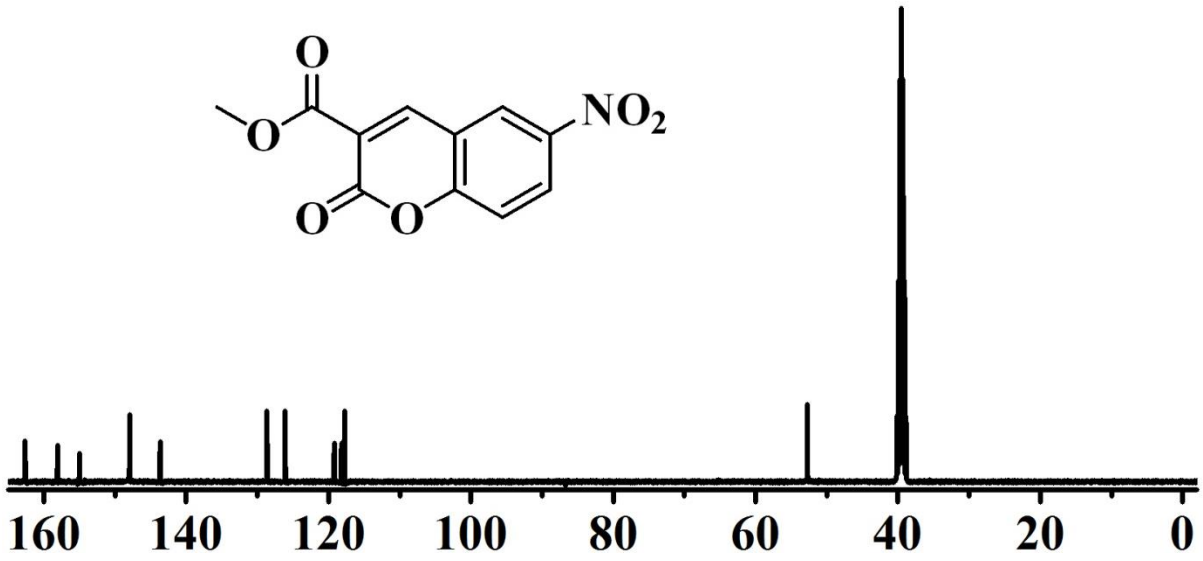

Fig. S14: ^{13}C NMR (100 MHz, DMSO-d_6, δ in ppm, 298K) spectra of Compound **5**.

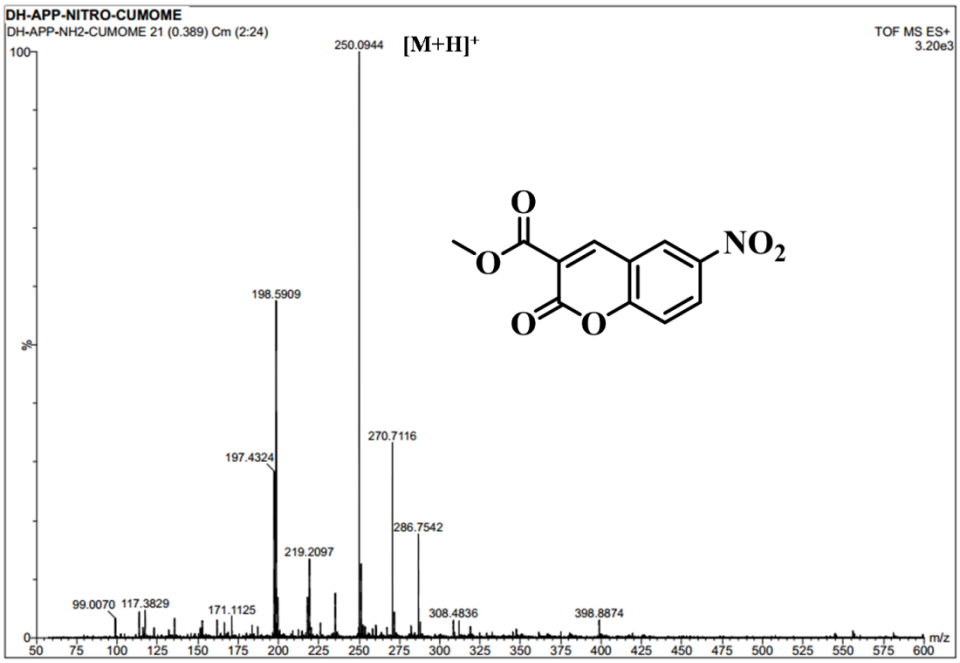

Fig. S15: Mass spectrum of Compound **5**.

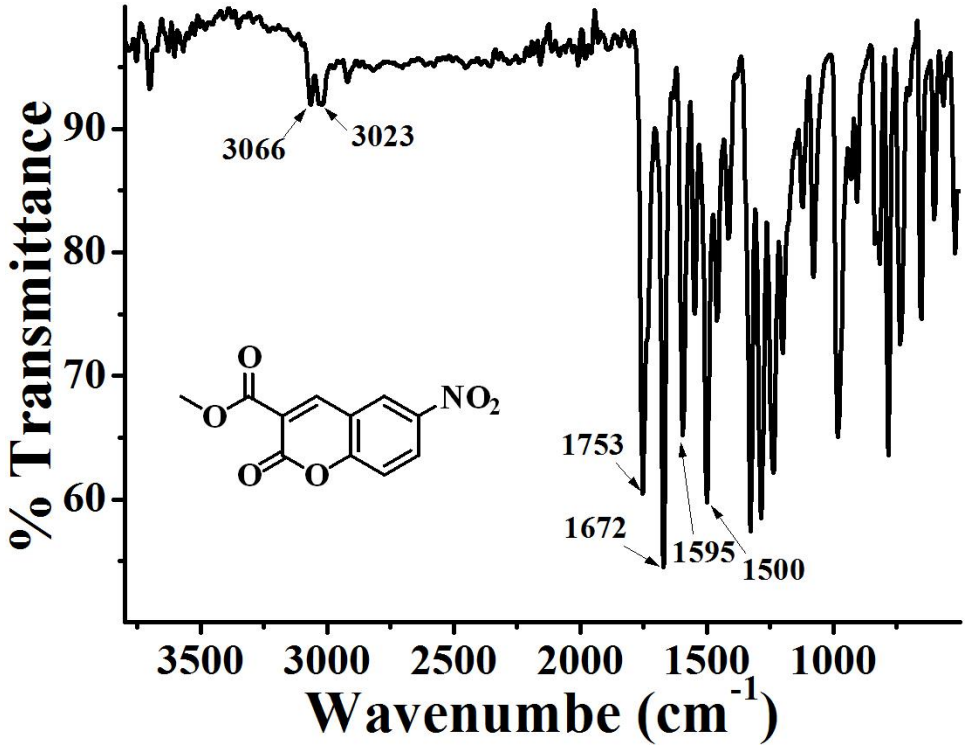

Fig. S16: FT-IR spectrum of Compound **5**.

(c). Synthesis of 6-nitro coumarin-3-carboxylic acid 6:

To 2.50 g (10 mmol) of compound **5**, 40 mL MeOH and 2(M) 16 mL NaOH were added and the progress of saponification was monitored by thin layer chromatography (TLC). The reaction mixture was stirred. After 10 h, methanol was removed under vacuum; the residue was dissolved in 50 mL of water and washed with diethyl ether (2 X 50 mL). Then the pH of the aqueous layer was adjusted to 2 using 1 (M) HCl and it was extracted with ethyl acetate (3 X 50 mL). The extracts were pooled, dried over anhydrous sodium sulfate, and evaporated under vacuum to obtain compound as a yellowish powder.

Yield: 2.31 g (9.32 mmol, 92.87%)

^{1}H NMR (400 MHz, DMSO-d_6, δ in ppm): 13.90-12.54 (br, 1H, -COOH), 8.93-8.78 (m, 2H, Ar-H), 8.50-8.37 (m, 1H, Ar-H), 7.66-7.51 (m, 1H, Ar-H). ^{13}C NMR (100 MHz, DMSO-d_6, δ in ppm): 164.71, 158.20, 147.60, 143.82, 128.94, 126.53, 124.96, 120.68, 118.35, 117.56. HR-ESI-MS (m/z): $[M+Na]^+$ calculated for $C_{10}H_5NO_6Na$ = 258.0015, found 258.0263.

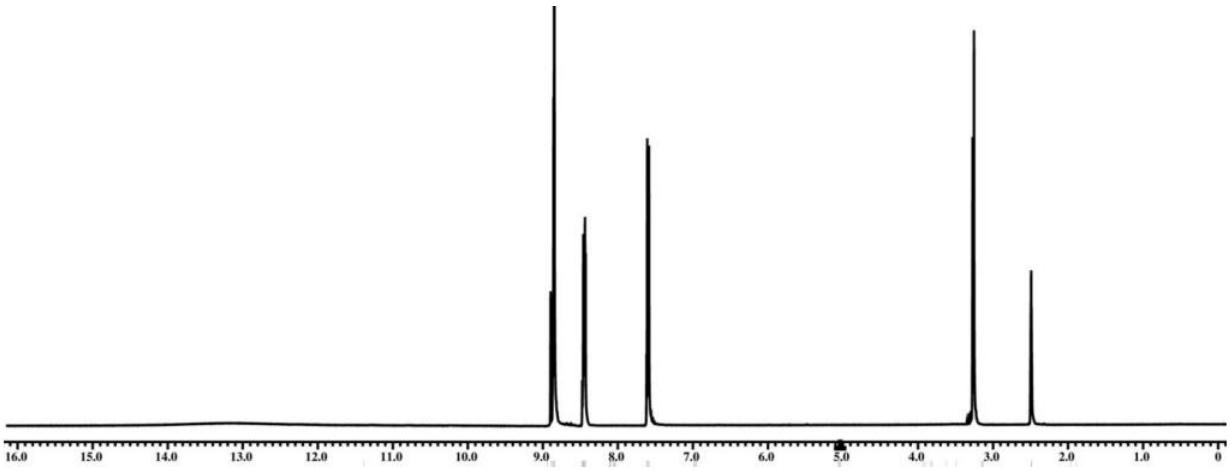

Fig. S17: ^{1}H NMR (400 MHz, DMSO-d_6, δ in ppm, 298K) spectra of Compound **6**.

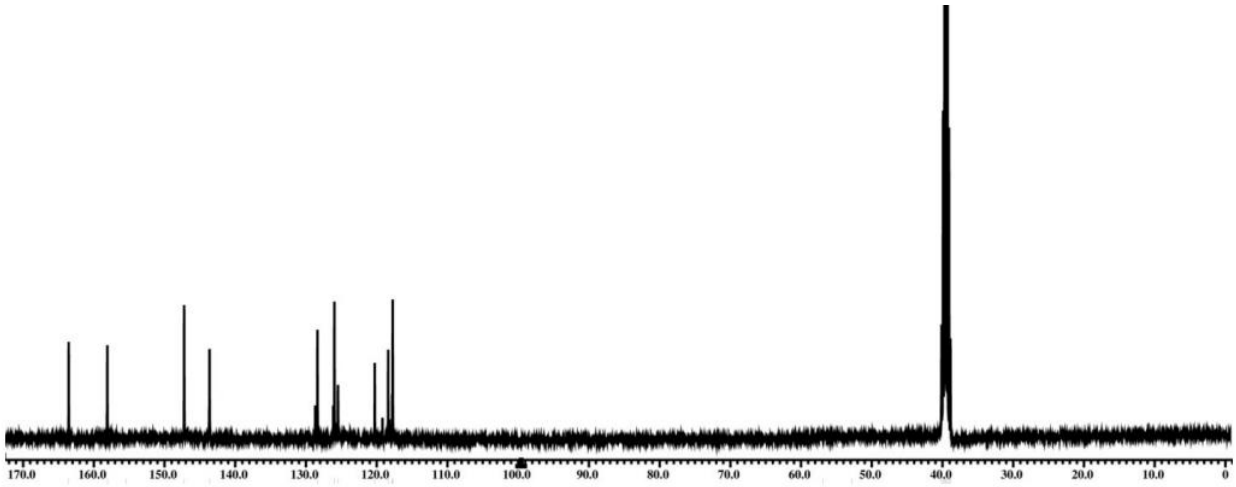

Fig. S18: ^{13}C NMR (100 MHz, DMSO-d_6, δ in ppm, 298K) spectra of Compound **6**.

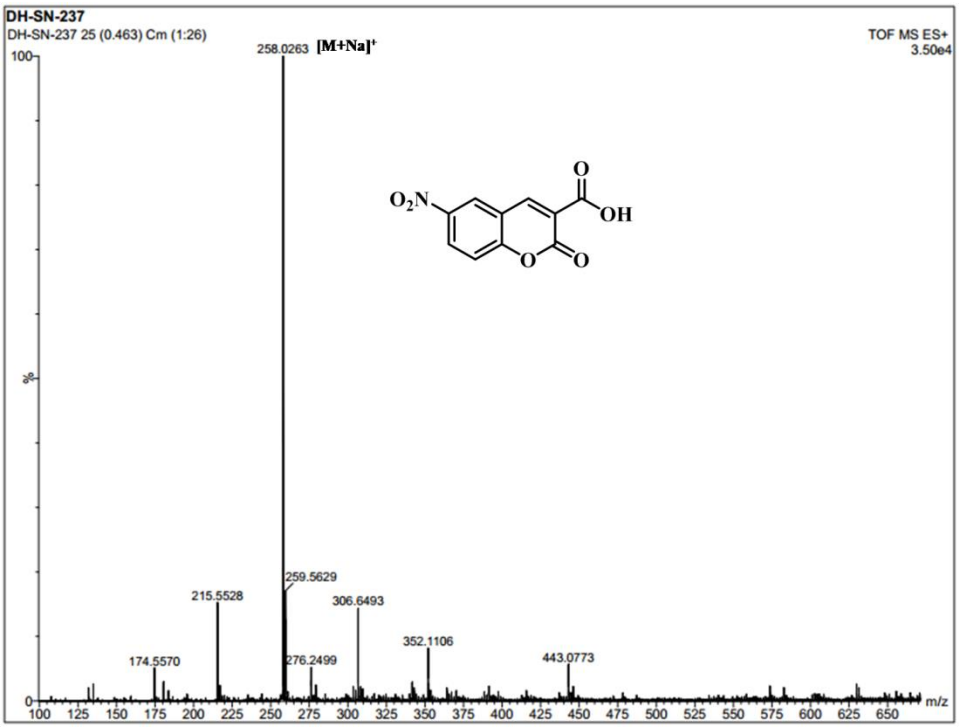

Fig. S19: Mass spectrum of Compound **6**.

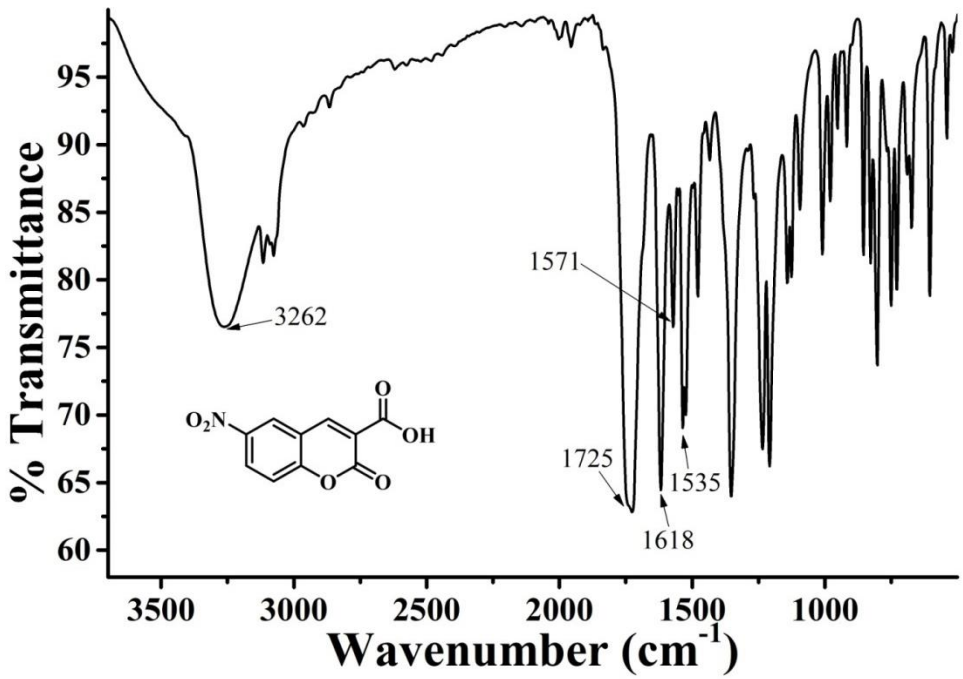

Fig. S20: FT-IR spectrum of Compound **6**.

(d). Synthesis of CouPheOMe (1):

1.17 g (5 mmol) 6-nitro coumarin-3-carboxylic acid **6** was dissolved in 30 mL of DCM and 5 mL of DMF in an ice-water bath. L-NH_2-Phe-OMe 1.25 g (7 mmol) was isolated from the corresponding methyl ester hydrochloride by neutralization and subsequent extraction with ethyl acetate and the ethyl acetate extract was concentrated under vacuum to 5 mL, then diluted with DCM to 30 mL. Then it was added to the reaction mixture, followed immediately by 1.45 g (7 mmol) of N,N′-dicyclohexylcarbodiimide (DCC) and 0.95 g (7 mmol) of HOBt. The reaction mixture was allowed to come to room temperature and then stirred for 48h. After that DCM was evaporated, the residue was taken in 30 mL ethyl acetate and N,N′-dicyclohexylurea (DCU) was filtered off. The organic layer was washed with 2(M) HCL (3X50 mL), brine (2X50 mL), then 1 (M) sodium carbonate (3X30 mL) and brine (2X30 mL) and dried over anhydrous sodium sulfate and evaporated under vacuum to yield the compound **1** as a white solid. Purification was done by silica gel column (100-200 mesh size) with an ethyl acetate and hexane mixture 1:2 as the eluent.

Yield: 1.60 g (4.01 mmol, 80 %).

^{1}H NMR (400 MHz, $CDCl_3$, δ in ppm, 298K): 8.99 (s, 1H, Phe NH), 8.91 (s, 1H, Ar-H), 8.58 (s, 1H, Ar-H), 8.50 (d, *J= 9.2*, 1H, Ar-H), 7.53 (d, *J= 9.2*, 1H, Ar-H), 5.01-4.96 (m, 1H, Phe C^{α} H), 3.76 (s, 3H, OCH_3), 1.30-1.26 (m, 1H, C^{β} H), 1.20-1.15 (m, 1H, C^{β} H). ^{13}C NMR (100 MHz, $CDCl_3$, δ in ppm, 298K): 171.41, 160.21, 159.74, 157.66, 147.37, 135.83, 129.34, 128.87, 128.59, 127.44, 125.59, 120.35, 118.63, 118.13, 54.49, 49.55, 33.88. ESI-MS (MeOH): m/z (Calc): $C_{20}H_{16}N_2O_7Na$ $[M+Na]^+$ 419.0855; found: 419.1111.

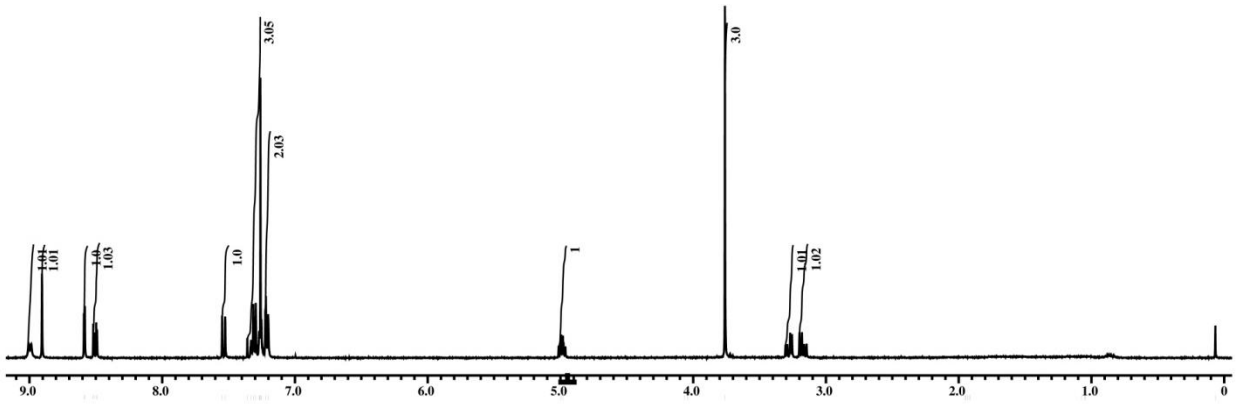

Fig. S21: ^{1}H NMR (400 MHz, $CDCl_3$, δ in ppm, 298K) spectra of Compound **1**.

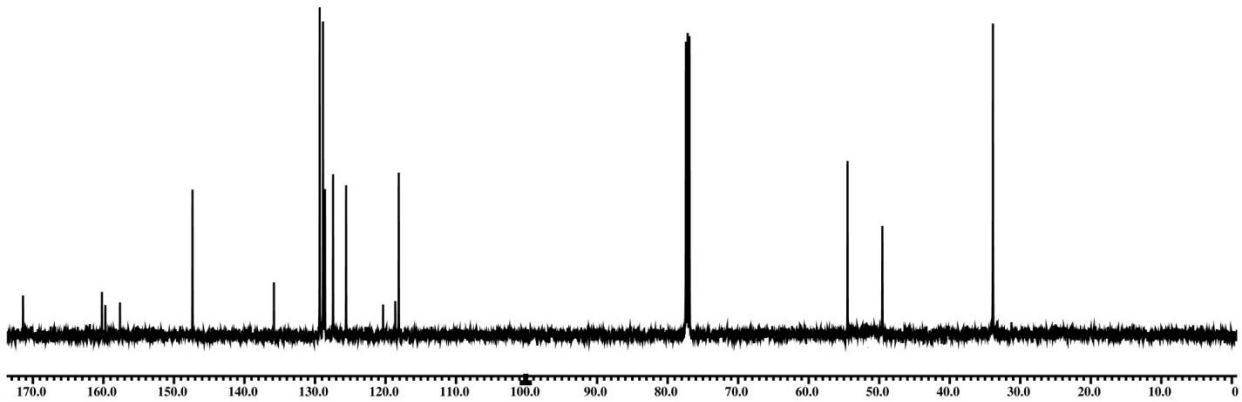

Fig. S22: ^{13}C NMR (100 MHz, $CDCl_3$, δ in ppm, 298K) spectra of Compound **1**.

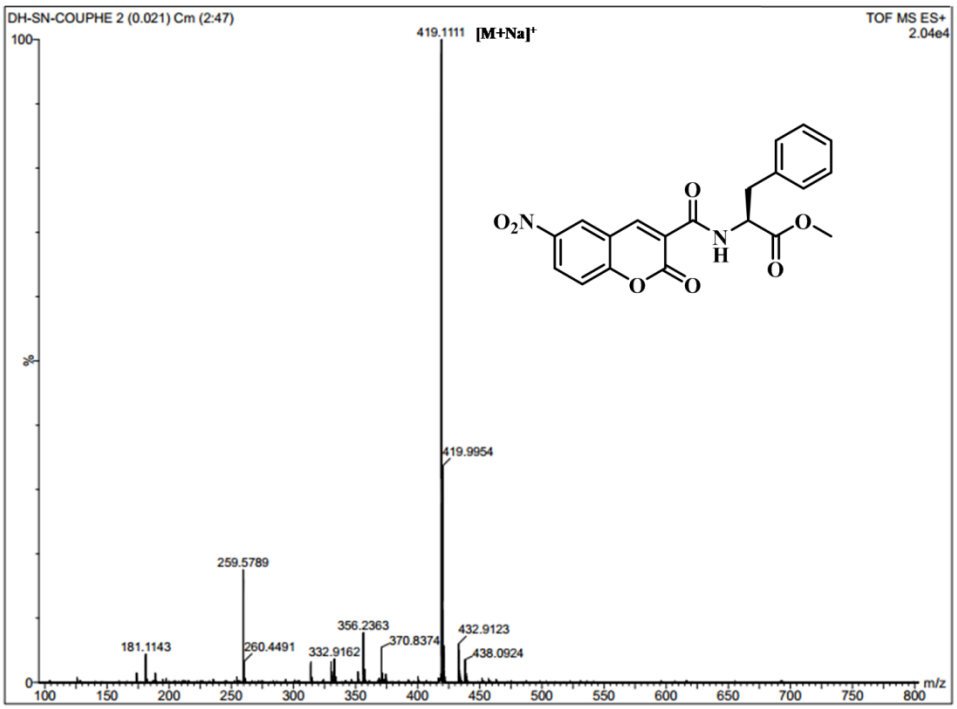

Fig. S23: Mass spectrum of Compound **1**.

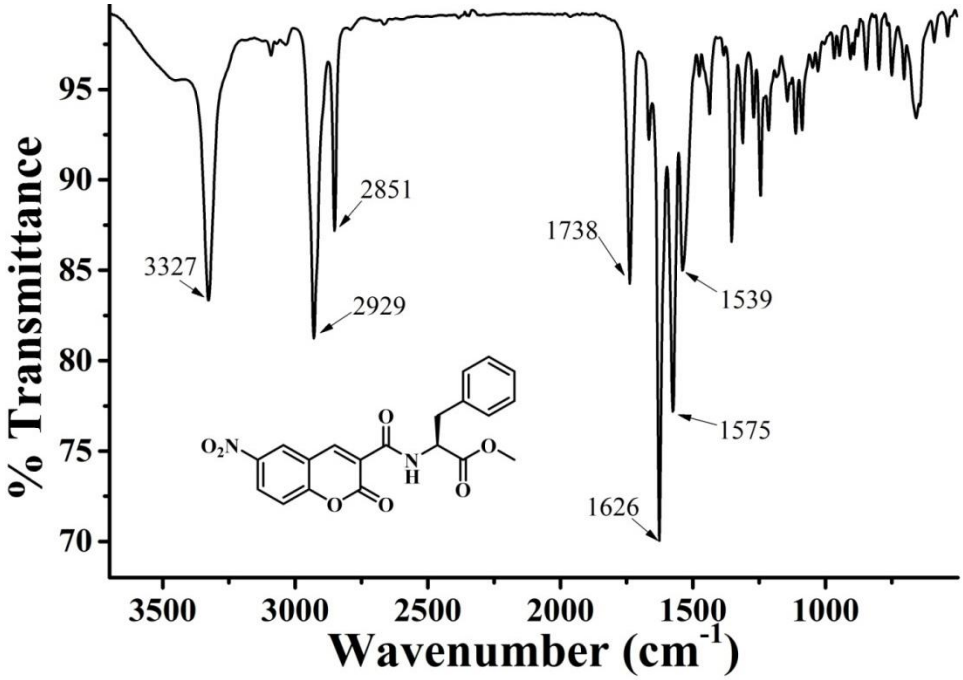

Fig. S24: FT-IR spectrum of Compound **1**.

(f). Synthesis of CouAlaOMe (2):

1.17 g (5 mmol) 6-nitro coumarin-3-carboxylic acid **6** was dissolved in 30 mL of DCM and 5 mL of DMF in an ice-water bath. L-NH_2-Ala-OMe 0.72 g (7 mmol) was isolated from the corresponding methyl ester hydrochloride by neutralization and subsequent extraction with ethyl acetate and the ethyl acetate extract was concentrated under vacuum to 5 mL, then diluted with DCM to 30 mL. Then it was added to the reaction mixture, followed immediately by 1.45 g (7 mmol) of N,N′-dicyclohexylcarbodiimide (DCC) and 0.95 g (7 mmol) of HOBt. The reaction mixture was allowed to come to room temperature and then stirred for 48h. After that DCM was evaporated, the residue was taken in 30 mL ethyl acetate and N,N′-dicyclohexylurea (DCU) was filtered off. The organic layer was washed with 2(M) HCL (3X50 mL), brine (2X50 mL), then 1 (M) sodium carbonate (3X30 mL) and brine (2X30 mL) and dried over anhydrous sodium sulfate and evaporated under vacuum to yield the compound **2** as a white solid. Purification was done by silica gel column (100-200 mesh size) with an ethyl acetate and hexane mixture 1:2 as the eluent.

Yield: 1.17 g (3.65 mmol, 73 %).

^{1}H NMR (400 MHz, $CDCl_3$, δ in ppm, 298K): 9.06 (s, 1H, Ala NH), 8.96 (s, 1H, Ar-H), 8.61 (s, 1H, Ar-H), 8.52 (d, *J= 9.2*, 1H, Ar-H), 7.56 (d, *J= 9.2*, 1H, Ar-H), 4.80-4.73 (m, 1H, Ala C^{α} H), 3.80 (s, 3H, OCH_3), 1.56 (d, J=7.32, 3H, Ala CH_3). ^{13}C NMR (100 MHz, $CDCl_3$, δ in ppm, 298K): 172.73, 160.05, 157.66, 147.44, 144.72, 128.59, 125.62, 120.40, 118.66, 118.07, 52.74, 48.94, 18.16. ESI-MS (MeOH): m/z (Calc): $C_{14}H_{12}N_2O_7Na$ $[M+Na]^+$ 343.0542; found: 343.0890.

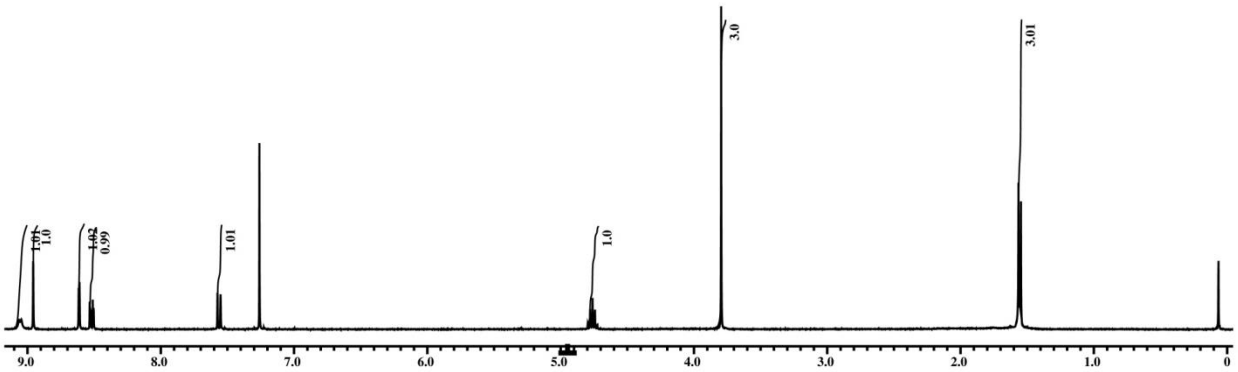

Fig. S25: ^{1}H NMR (400 MHz, $CDCl_3$, δ in ppm, 298K) spectra of Compound **2**.

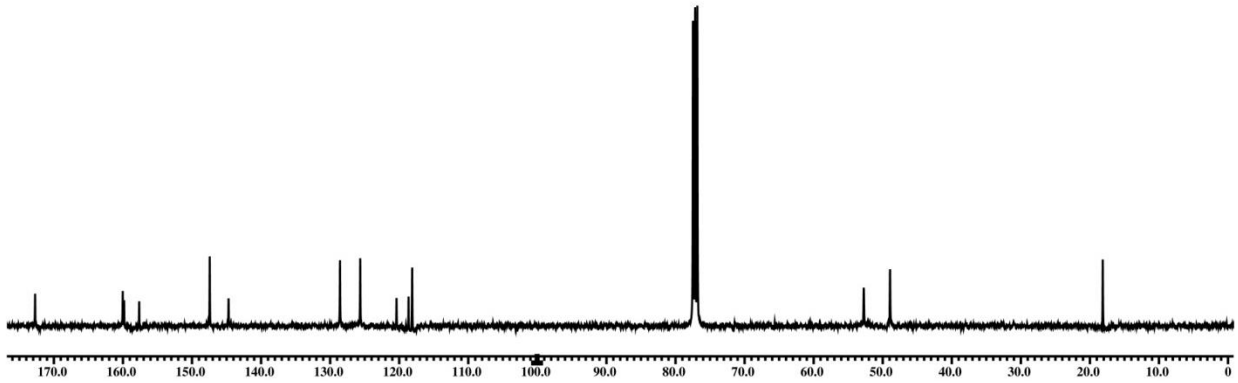

Fig. S26: ^{13}C NMR (100 MHz, $CDCl_3$, δ in ppm, 298K) spectra of Compound **2**.

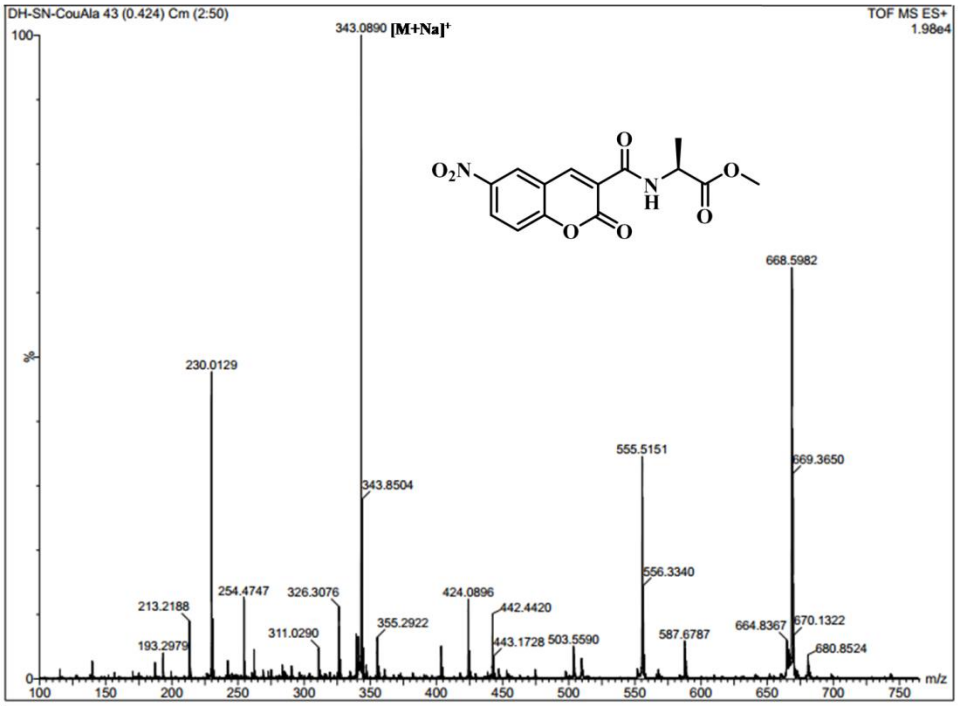

Fig. S27: Mass spectrum of Compound **2**.

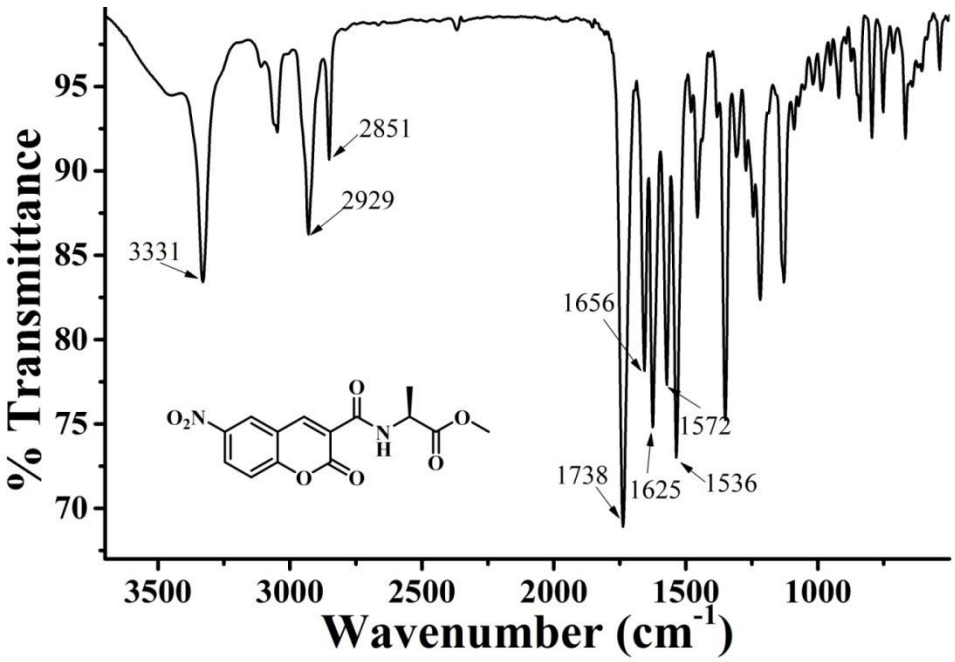

Fig. S28: FT-IR spectrum of Compound **2**.

(e). Synthesis of CouLeuOMe (3):

1.17 g (5 mmol) 6-nitro coumarin-3-carboxylic acid **6** was dissolved in 30 mL of DCM and 5 mL of DMF in an ice-water bath. L-NH_2-Leu-OMe 1.02 g (7 mmol) was isolated from the corresponding methyl ester hydrochloride by neutralization and subsequent extraction with ethyl acetate and the ethyl acetate extract was concentrated under vacuum to 5 mL, then diluted with DCM to 30 mL. Then it was added to the reaction mixture, followed immediately by 1.45 g (7 mmol) of N,N′-dicyclohexylcarbodiimide (DCC) and 0.95 g (7 mmol) of HOBt. The reaction mixture was allowed to come to room temperature and then stirred for 48h. After that DCM was evaporated, the residue was taken in 30 mL ethyl acetate and N,N′-dicyclohexylurea (DCU) was filtered off. The organic layer was washed with 2(M) HCL (3X50 mL), brine (2X50 mL), then 1 (M) sodium carbonate (3X30 mL) and brine (2X30 mL) and dried over anhydrous sodium sulfate and evaporated under vacuum to yield the compound **3** as a white solid. Purification was done by silica gel column (100-200 mesh size) with an ethyl acetate and hexane mixture 1:2 as the eluent.

Yield: 1.56 g (4.31 mmol, 86 %).

^{1}H NMR (400 MHz, $CDCl_3$, δ in ppm, 298K): 8.97 (s, 1H, Ar-H), 8.90 (s, 1H, Ala NH), 8.62 (s, 1H, Ar-H), 8.50 (d, *J= 9.2*, 1H, Ar-H), 7.55 (d, *J= 9.2*, 1H, Ar-H), 4.78-4.73 (m, 1H, Leu C^{α} H), 3.74 (s, 3H, OCH_3), 1.77-1.69 (m, 3H, C^{β} H & C^{γ} H), 0.95 (d, J=5.08, 6H, Leu CH_3). ^{13}C NMR (100 MHz, $CDCl_3$, δ in ppm, 298K): 172.66, 160.33, 159.92, 157.61, 147.52, 144.69, 128.55, 125.64, 120.33, 118.65, 118.10, 52.53, 51.68, 41.10, 25.11, 22.91, 21.90. ESI-MS (MeOH): m/z (Calc): $C_{17}H_{18}N_2O_7Na$ $[M+Na]^+$ 385.1012; found: 385.1160.

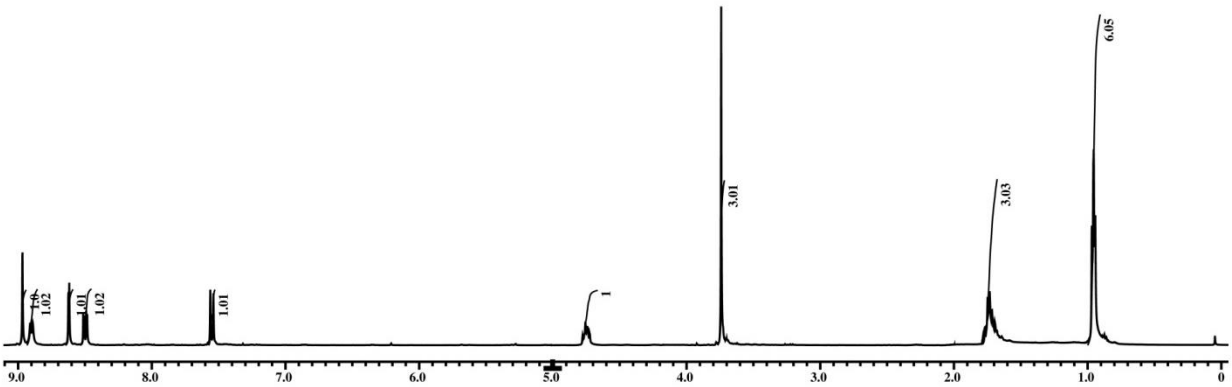

Fig. S29: ^{1}H NMR (400 MHz, $CDCl_3$, δ in ppm, 298K) spectra of Compound **3**.

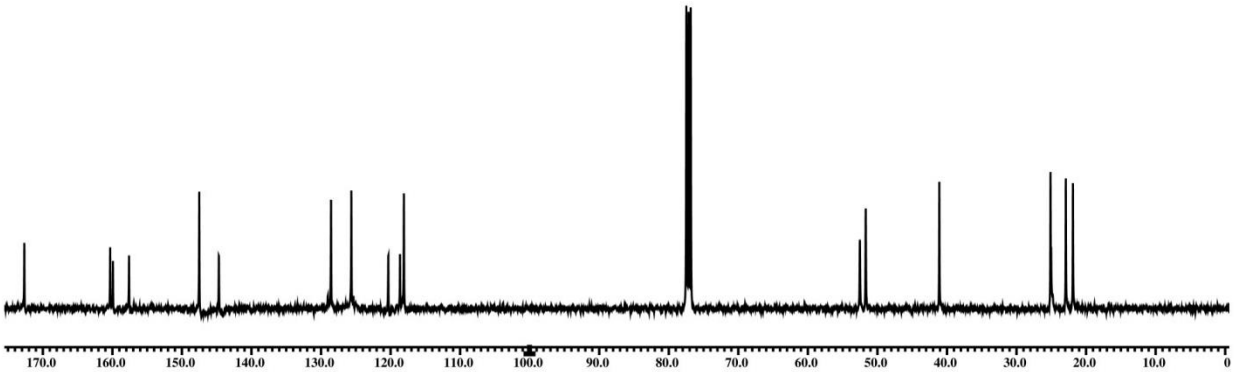

Fig. S30: ^{13}C NMR (100 MHz, $CDCl_3$, δ in ppm, 298K) spectra of Compound **3**.

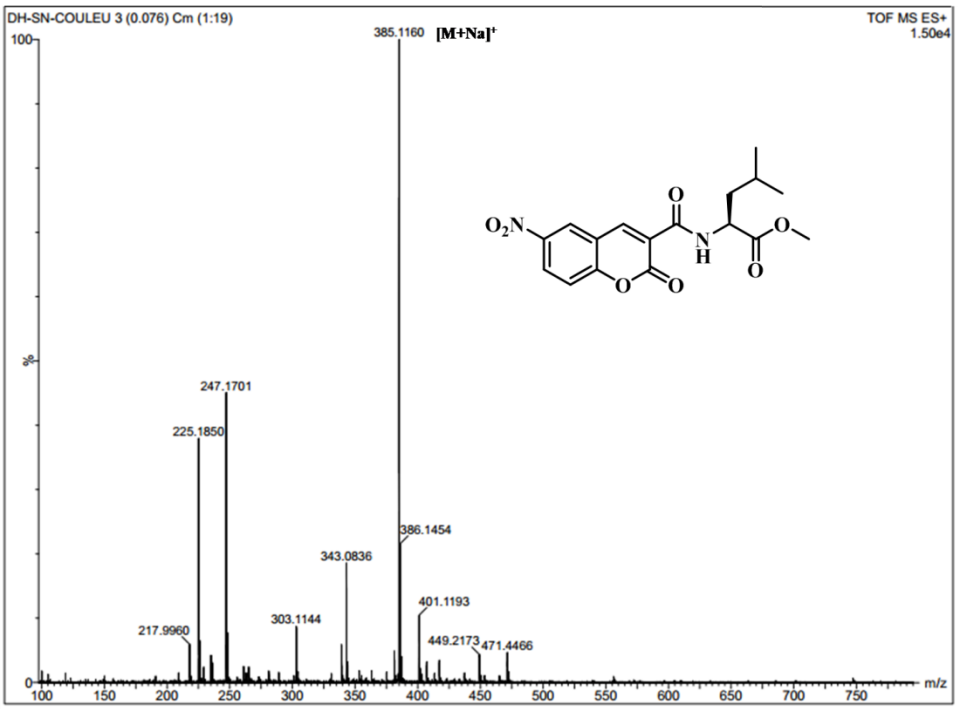

Figure S31: Mass spectrum of Compound **3**.

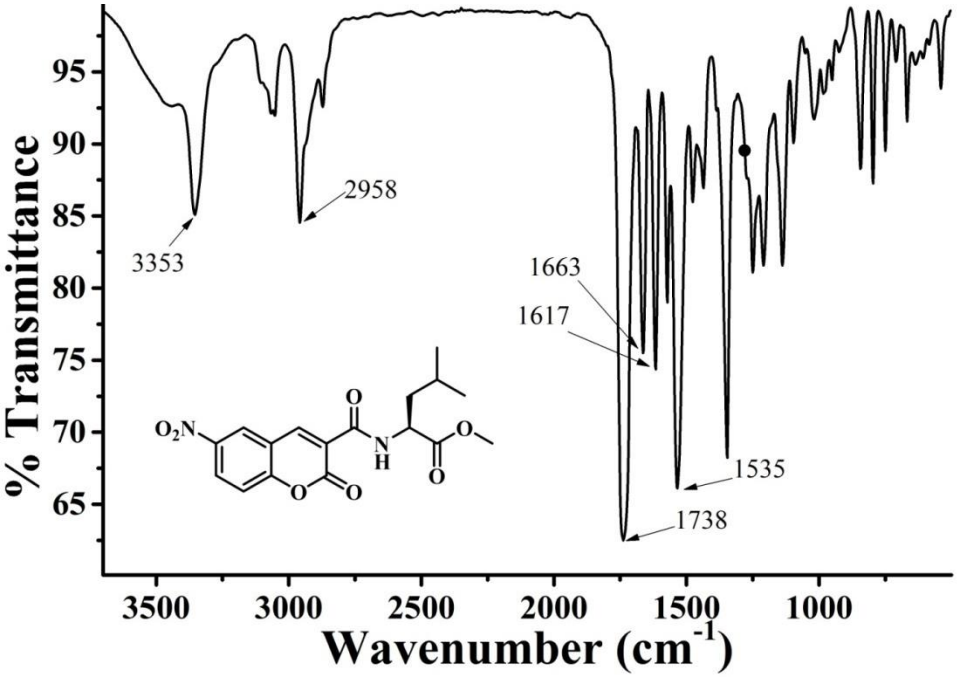

Fig. S32: FT-IR spectrum of Compound **3**.

References:

1 J. F. Nye, *Physical Properties of Crystals: Their Representation by Tensors and Matrices*, Oxford University Press, London, 1985, pp. 250-251.

2 A. Yariv, *Quantum electronics*, Wiley, New York, 1989, pp. 381-382.

3 R. W. Boyd, *Nonlinear Optics*, Academic Press, London, 2008, pp. 46-48.